⌘ *Author's Choice*

Porphyrins Promote the Association of GENOMES UNCOUPLED 4 and a Mg-chelatase Subunit with Chloroplast Membranes*⑤

Neil D. Adhikari[‡§]**, Robert Orler**[‡1]**, Joanne Chory**[¶]**, John E. Froehlich**[‡1]**, and Robert M. Larkin**[‡‖2]

From the ‡Department of Energy Plant Research Laboratory, §Genetics Program, and ‖Department of Biochemistry and Molecular Biology, Michigan State University, East Lansing, Michigan 48824 and the ¶Howard Hughes Medical Institute and Plant Biology Laboratory, Salk Institute for Biological Studies, La Jolla, California 92037

In plants, chlorophylls and other tetrapyrroles are synthesized from a branched pathway that is located within chloroplasts. GUN4 (GENOMES UNCOUPLED 4) stimulates chlorophyll biosynthesis by activating Mg-chelatase, the enzyme that commits porphyrins to the chlorophyll branch. GUN4 stimulates Mg-chelatase by a mechanism that involves binding the ChlH subunit of Mg-chelatase, as well as a substrate (protoporphyrin IX) and product (Mg-protoporphyrin IX) of Mg-chelatase. We chose to test whether GUN4 might also affect interactions between Mg-chelatase and chloroplast membranes, the site of chlorophyll biosynthesis. To test this idea, we induced chlorophyll precursor levels in purified pea chloroplasts by feeding these chloroplasts with 5-aminolevulinic acid, determined the relative levels of GUN4 and Mg-chelatase subunits in soluble and membrane-containing fractions derived from these chloroplasts, and quantitated Mg-chelatase activity in membranes isolated from these chloroplasts. We also monitored GUN4 levels in the soluble and membrane-containing fractions derived from chloroplasts fed with various porphyrins. Our results indicate that 5-aminolevulinic acid feeding stimulates Mg-chelatase activity in chloroplast membranes and that the porphyrin-bound forms of GUN4 and possibly ChlH associate most stably with chloroplast membranes. These findings are consistent with GUN4 stimulating chlorophyll biosynthesis not only by activating Mg-chelatase but also by promoting interactions between ChlH and chloroplast membranes.

Chlorophylls are produced from a branched pathway located within plastids that also produces heme, siroheme, and phytochromobilin. In photosynthetic organisms, the universal tetrapyrrole precursor 5-aminolevulinic acid (ALA)[3] is derived from glutamyl-tRNA and subsequently converted into protoporphyrinogen IX in the chloroplast stroma. Protoporphyrinogen IX is converted to protoporphyrin IX (PPIX) and then ultimately to chlorophylls on plastid membranes. Almost all the genes encoding chlorophyll biosynthetic enzymes have been identified. Transcriptional control provides coarse regulation of this pathway, and the regulation of enzyme activities provides fine regulation (1, 2).

Arabidopsis GUN4 (hereafter referred to as GUN4) was identified from a screen for plastid-to-nucleus signaling mutants (3–5). GUN4 is a major positive regulator of chlorophyll biosynthesis but is not absolutely required for the accumulation of chlorophyll in Arabidopsis (5). In *Synechocystis,* one of the GUN4 relatives, *sll0558* (hereafter referred to as SynGUN4), was subsequently shown also to be required for the accumulation of chlorophyll (6, 7). The 140-kDa subunit of Mg-chelatase copurifies with the 22-kDa GUN4 from solubilized Arabidopsis thylakoid membranes (5); similar results were subsequently reported using *Synechocystis* (7). Mg-chelatase catalyzes the insertion of Mg^{2+} into PPIX, yielding Mg-protoporphyrin IX (Mg-PPIX). This reaction diverts PPIX from heme biosynthesis and commits this porphyrin to chlorophyll biosynthesis. Mg-chelatase requires three subunits *in vitro* and *in vivo*. These three subunits are conserved from prokaryotes to plants and are commonly referred to as BchH or ChlH, BchD or ChlD, and BchI or ChlI. In Arabidopsis, these subunits are 140, 79, and 40 kDa, respectively. ChlH is the porphyrin-binding subunit and is likely the Mg^{2+}-binding subunit of Mg-chelatase. ChlI and ChlD are related to AAA-type ATPases and form two associating hexameric rings that interact with ChlH and drive the ATP-dependent metalation of PPIX (8, 9). SynGUN4 stimulates *Synechocystis* Mg-chelatase (5, 10, 11). Cyanobacterial relatives of GUN4 bind deuteroporphyrin IX (DPIX) and Mg-deuteroporphyrin IX (Mg-DPIX) (5, 10, 11), which are more water-soluble derivatives of PPIX and Mg-PPIX. Crystal structures of SynGUN4 and *Thermosynechococcus elongatus* GUN4 indicate a novel fold that resembles a "cupped hand" that binds DPIX and Mg-DPIX (10, 11). Preincubation experiments indicate that a SynGUN4-DPIX complex

[3] The abbreviations used are: ALA, 5-aminolevulinic acid; DPIX, deuteroporphyrin IX; LHCP, light-harvesting chlorophyll *a/b*-binding protein; GST, glutathione *S*-transferase, GUN4, GENOMES UNCOUPLED 4; Mg-DPIX, Mg-deuteroporphyrin IX; Mg-PPIX, Mg-protoporphyrin IX; Mg-PPIX MT, Mg-PPIX methyl transferase; ORF, open reading frame; PO, protoporphyrinogen IX oxidase; PPIX, protoporphyrin IX; SS, the small subunit of ribulose-bisphosphate carboxylase/oxygenase; Tic40, Translocon at the inner envelope 40; Ni-NTA, nickel-nitrilotriacetic acid; DTT, dithiothreitol; MOPS, 4-morpholinepropanesulfonic acid; Tricine, *N*-[2-hydroxy-1,1-bis(hydroxymethyl)ethyl]glycine; Mg-PPIX ME, Mg-protoporphyrin IX monomethyl ester.

stimulates Mg-chelatase more potently than SynGUN4 (5). SynGUN4 was found to lower the K_m^{DPIX} of *Synechocystis* Mg-chelatase (10) and to cause a striking increase in the apparent first-order rate constant for DPIX-Mg-chelatase interactions, an effect that is particularly striking at low Mg^{2+} concentrations (11). The Mg-DPIX binding activity of SynGUN4 was also found to be essential for stimulating Mg-chelatase (10).

GUN4 and Mg-chelatase subunits have been found in both soluble and membrane-containing fractions of purified chloroplasts (5, 12–15). In contrast, protoporphyrinogen IX oxidase (PO) and Mg-PPIX methyltransferase (Mg-PPIX MT), which function immediately upstream and downstream of Mg-chelatase in the chlorophyll biosynthetic pathway, are found only in the membrane-containing fractions and not in stromal fractions when purified chloroplasts are lysed and fractionated (16–20). PPIX and Mg-PPIX accumulate in chloroplast membranes rather than soluble fractions, which provides more evidence that these chlorophyll precursors are synthesized on chloroplast membranes (21). If GUN4 promotes chlorophyll biosynthesis by not only stimulating Mg-chelatase activity but also promoting the formation of enzyme complexes that channel porphyrins into chlorophyll biosynthesis, GUN4 would be expected to more stably associate with chloroplast membranes by interacting with chloroplast membrane lipids or chlorophyll biosynthetic enzymes after binding porphyrins. In the following, we provide experimental evidence supporting this model.

EXPERIMENTAL PROCEDURES

Construction of Plasmids and Strains—For *in vitro* transcription/translation experiments, the entire GUN4 open reading frame (ORF) was amplified from bacterial artificial chromosome clone T1G3 (Arabidopsis Biological Resource Center, Ohio State University, Columbus) using CGGGATCCTATCTTCCCCTGACGTGAC, AACTGCAGAAAGACATCAGAAGCTGTAATTTG, and *PfuTurbo*® DNA polymerase (Stratagene, La Jolla CA). The resulting PCR product was ligated into pCMX-PL1 (22) between BamHI and PstI. *In vitro* transcription and translation of the control protein translocon at the inner envelope 40 (Tic40), the small subunit of ribulose-bisphosphate carboxylase/oxygenase (SS), and a light-harvesting chlorophyll *a/b*-binding protein (LHCP) were as described previously (23, 24). A glutathione *S*-transferase (GST)-tagged GUN4 deletion mutant that lacks the predicted 69-residue transit peptide (GST-GUN4 Δ1–69) was used for the expression and purification of GUN4 from *Escherichia coli*, as described previously (5). Site-directed mutagenesis was performed on each of these plasmids using the QuickChange® XL site-directed mutagenesis kit (Stratagene) and oligonucleotides that were designed according to the manufacturer's recommendations (supplemental Table 1). All mutations were confirmed by sequencing at the Research Technology Support Facility (Michigan State University, East Lansing, MI).

Isolation of Pea Chloroplasts—Intact chloroplasts were isolated from 6- to 8-day-old pea seedlings and purified over a Percoll gradient as described previously (25). Intact pea chloroplasts were reisolated and resuspended in import buffer (330 mM sorbitol, 50 mM HEPES-KOH, pH 8.0) at a chlorophyll concentration of 1 mg/ml. Protein import was performed as described previously (25).

In Vitro Translation of Precursor Protein—All precursor proteins used in this study were either radiolabeled with [^{35}S]methionine or [^{3}H]leucine and translated with the T$_N$T® Coupled Reticulocyte Lysate System (Promega, Madison WI) according to the manufacturer's recommendations.

Import Assays—Large scale import assays contained 50 mM HEPES-KOH, pH 8.0, 330 mM sorbitol, 4 mM Mg-ATP, 100 μl of chloroplasts with a chlorophyll concentration of 1 mg/ml, and labeled precursor protein at a final volume of 300 μl. After a 30-min incubation at room temperature under white light provided by broad spectrum fluorescent tube lamps at 75 μmol m^{-2} s^{-1}, the import assay was divided into two 150-μl aliquots. One aliquot was not further treated. For this aliquot, intact chloroplasts were directly recovered by centrifugation through a 40% Percoll cushion. The remaining aliquot was incubated with trypsin for 30 min on ice as described previously (26). After stopping the protease treatment with trypsin inhibitor as described previously (26), we again recovered chloroplasts by centrifugation through a 40% Percoll cushion. Recovered intact chloroplasts were resuspended in 200 μl of lysis buffer (25 mM HEPES-KOH, pH 8.0, 4 mM MgCl$_2$), incubated on ice for 20 min, and then fractionated into a soluble and membrane-containing pellet fraction by centrifugation at 16,000 × g for 5 min. The pellet fraction contains the outer envelope, inner envelope, and thylakoid membranes. All fractions were analyzed using SDS-PAGE and subjected to fluorography. Fluorograms were exposed to x-ray film (Eastman Kodak Co.) for 1–7 days. Import assays were quantitated by scanning developed films with the VersaDoc 4000 MP Imaging System and Quantity One software, as recommended by the manufacturer (Bio-Rad).

ALA and Porphyrin Feeding—Prior to import, intact chloroplasts were incubated in import buffer (330 mM sorbitol, 50 mM HEPES-KOH, pH 8.0) that contained or lacked 10 mM ALA (Sigma) for 15 min at 26 °C in the dark, unless indicated otherwise. PPIX, Mg-PPIX, uroporphyrin III, coproporphyrin III, hemin, and pheophorbide *a* were all purchased from Frontier Scientific (Logan, UT). These porphyrins were first dissolved in DMSO, and their concentrations were determined spectrophotometrically as described previously (27–30). These stock solutions were diluted with import buffer, giving final porphyrin concentrations of 20 μM and final DMSO concentrations of 1–2%. Intact chloroplasts were incubated in these solutions exactly as described for ALA.

Fractionation of Chloroplasts into Stroma, Thylakoid, and Envelope Fractions—Fractionation of chloroplasts was performed as described previously (31), with modifications. First, large scale import assays were performed with (+) or without (−) an ALA pretreatment as described above. After import, intact chloroplasts were recovered by centrifugation through a 40% Percoll cushion. The intact chloroplasts were then resuspended in 0.6 M sucrose containing 25 mM HEPES-KOH, pH 8.0, 2 mM MgCl$_2$, 8 mM EDTA. The suspension was placed on ice for 20 min and then placed at −20 °C overnight. Subsequently, the suspension was thawed at room temperature, gently mixed, and then diluted with 2 volumes of dilution buffer (25 mM HEPES-KOH, pH 8.0, 2 mM MgCl$_2$, 8 mM EDTA). This

suspension was then centrifuged at $1,500 \times g$ for 5 min. The resulting pellet predominantly contained the thylakoid fraction and was diluted 2-fold with $2\times$ SDS-PAGE loading buffer (32). The remaining supernatant was then centrifuged at $100,000 \times g$ for 1 h. The resulting pellet fraction predominantly contained envelopes and was diluted 2-fold in $2\times$ SDS-PAGE loading buffer. Cold acetone was added to the supernatant fraction to a final concentration of 80%, incubated on ice for 30 min, and then centrifuged at $15,000 \times g$ for 5 min. The precipitated soluble protein fraction was resuspended in $2\times$ SDS-PAGE loading buffer. All fractions were analyzed by SDS-PAGE.

Analysis of Porphyrins in Purified Chloroplasts—PPIX and Mg-PPIX levels in purified chloroplasts were quantitated following ALA feeding and mock protein import. 0.1-ml aliquots of chloroplasts were collected by centrifugation at $1,900 \times g$ for 5 min at 4 °C through a 40% Percoll cushion. Recovered chloroplasts were lysed by resuspension in 700 μl of acetone, 0.1 M NH_4OH (9:1, v/v). These lysates were clarified by centrifugation at $16,000 \times g$ for 10 min at 4 °C. Chlorophyll was removed from the resulting supernatants by hexane extraction as described previously (28). We quantitated the amount of PPIX and Mg-PPIX in these hexane-extracted supernatants using fluorescence spectroscopy with a QuantaMaster™ spectrofluorometer (Photon Technology International, Inc., London Ontario) as described previously (28). PPIX and Mg-PPIX, purchased from Frontier Scientific, were used to construct standard curves.

Quantitative Analysis of Porphyrin Binding—GUN4 $\Delta1$–69 and versions of GUN4 $\Delta1$–69 that contain amino acid substitutions were expressed and purified from *E. coli* as described previously (5). Binding constants were measured by quantitating the quenching of tryptophan fluorescence in GUN4 $\Delta1$–69 by bound porphyrins essentially as described for the cyanobacterial relatives of GUN4 (5, 10, 11). Binding reactions were in 20 mM MOPS-KOH, pH 7.9, 1 mM DTT, 300 mM glycerol and contained 200 nM GUN4 $\Delta1$–69 or GUN4 $\Delta1$–69 with the indicated single amino acid changes and variable concentrations of DPIX and Mg-DPIX (Frontier Scientific). We determined binding constants for PPIX, Mg-PPIX, and Mg-PPIX ME, uroporphyrin III, coproporphyrin III, hemin, and pheophorbide *a* using the same conditions except that binding reactions also contained 1% DMSO. Stock solutions of DPIX and Mg-DPIX were prepared as described previously (33). Stock solutions of all other porphyrins were prepared as described under "ALA and Porphyrin Feeding." We calculated binding constants using DYNAFIT (34) as described previously (33). The data fit best with a model that predicts a single binding site.

Mg-chelatase Assays—Chloroplasts were purified from pea and subjected to hypotonic lysis as described above, except that lysis buffer also contained 1 mM DTT and 2 mM Pefabloc (Sigma). Supernatants were flash-frozen in liquid nitrogen and stored at −80 °C. We assayed pellet fractions for Mg-chelatase activity immediately by resuspending them in a Mg-chelatase assay buffer (50 mM Tricine-KOH, pH 7.8, 1 mM EDTA, 9 mM $MgCl_2$, 4 mM MgATP, 1 mM DTT, 0.25% bovine serum albumin, 5% glycerol, 60 mM phosphocreatine, 4 units/ml creatine phosphokinase) and incubating the resuspended pellets for 30 min at 30 °C as recommended previously (14, 35). PPIX dissolved in DMSO was added to particular reactions as indicated

in the text. The final concentrations of PPIX and DMSO were 1.5 μM and 2%, respectively, as recommended previously (36). Aliquots of 8 μl were removed at 5-min intervals during a 30-min incubation, diluted into 200 μl of acetone, 0.1 M NH_4OH (9:1, v/v), and vortexed to terminate the reaction. The terminated reactions were centrifuged for 10 min at $16,000 \times g$ at 4 °C. Mg-PPIX in the resulting supernatants was quantitated as described under "Quantitative Analysis of Porphyrin Binding." We subtracted the amount of Mg-PPIX in the membranes before the reactions were initiated from the amount of Mg-PPIX at the end of each time point. Three replicates were analyzed for each time point. Mg-PPIX accumulated linearly for the entire 30-min assay. To assay supernatants for Mg-chelatase activity, supernatants were rapidly thawed, clarified at $16,000 \times g$ at 4 °C for 10 min, and then concentrated nearly 5-fold using an Amicon ultracentrifugal filter device with a nominal molecular weight limit of 10,000 (Millipore, Billerica, MA). The concentrated supernatants were diluted into a concentrated Mg-chelatase assay buffer yielding the same assay conditions described for pellets. Reactions were initiated by adding 1.5 μM PPIX.

Polyclonal Anti-ChlH, Anti-ChlI, and Anti-ChlD Antibody Development—Poly(A)$^+$ mRNA was isolated from *Arabidopsis thaliana* (Columbia-0 ecotype) using the Absolutely mRNA kit (Stratagene). We prepared first-strand cDNA using Superscript II (Invitrogen). A cDNA encoding a 62-kDa fragment of ChlH that lacks the first 823 amino acid residues (ChlH $\Delta1$–823) was amplified from this first-strand cDNA as described for GUN4 $\Delta1$–69, except that CCGGAATTCGCTGTGGCCACACTG-GTCAAC and TCGCGTCGACTTATCGATCGATCCCT-TCGATCTTGTC were used. To express ChlH $\Delta1$–823 as a His-tagged protein in *E. coli*, this PCR product was ligated into pHIS8-3 (37) between EcoRI and SalI. The resulting plasmid was sequenced at the Research Technology Support Facility (Michigan State University) to confirm that no mutations were introduced during PCR. The His-tagged ChlH $\Delta1$–823 protein was expressed from the resulting plasmid in the *E. coli* strain BL21-CodonPlus® (DE3)-RIL (Stratagene) at 18 °C in Terrific Broth (32). We induced expression by adding 1 mM isopropyl β-D-1-thiogalactopyranoside (Sigma) when the A_{600} was 0.8. All subsequent steps were performed at 4 °C, unless indicated otherwise. Cells were harvested by centrifugation at $6,000 \times g$ for 10 min and resuspended in 20 ml of buffer A (50 mM Tris acetate, pH 7.9, 500 mM potassium acetate, 20 mM imidazole, 20 mM β-mercaptoethanol, 20% glycerol, 1% Triton X-100) per g of bacterial pellet. Cells were lysed by sonication. The resulting lysate was clarified by centrifugation at $10,000 \times g$ for 20 min. The supernatant was batch-bound to Ni-NTA-agarose (Qiagen, Valencia, CA) equilibrated in buffer A. Bound proteins were batch-washed twice with buffer A and twice with buffer A lacking Triton X-100. Ni-NTA-agarose was poured into an Econo-Pac column (Bio-Rad), and proteins were step-eluted using buffer B (20 mM Tris acetate, pH 7.9, 500 mM potassium acetate, 250 mM imidazole, 20 mM β-mercaptoethanol, 20% glycerol). Eluted proteins were dialyzed against buffer C (20 mM Tris acetate, pH 7.9, 150 mM potassium acetate, 2.5 mM $CaCl_2$, 20 mM β-mercaptoethanol, 20% glycerol), digested with thrombin (Sigma) at room temperature, and applied to the aforemen-

tioned Ni-NTA-agarose column equilibrated in buffer A. Proteins in the flow-through fraction were dialyzed against buffer D (20 mM Tris acetate, pH 7.9, 100 mM potassium acetate, 1 mM EDTA, 1 mM DTT, 20% glycerol), applied to a HiPrep™ 16/10 Q FF column (GE Healthcare) that was equilibrated in buffer D at a flow rate of 1.0 ml/min, and eluted with a 200-ml linear gradient to buffer E (20 mM Tris acetate, pH 7.9, 1000 mM potassium acetate, 1 mM EDTA, 1 mM DTT, 20% glycerol) also at a flow rate of 1.0 ml/min. Fractions of 2.5 ml containing ChlH Δ1–823 were pooled, concentrated using an Amicon Ultra-15 centrifugal filter unit with a nominal molecular weight limit of 30,000 (Millipore), dialyzed against storage buffer (50 mM Tricine-KOH, pH 7.9, 1 mM DTT, 50% glycerol), flash-frozen with liquid N_2, and stored in small aliquots at −80 °C. For polyclonal antibody development, purified ChlH Δ1–823 was dialyzed extensively against phosphate-buffered saline, pH 7.4 (32), and used to develop anti-ChlH Δ1–823 polyclonal antisera in New Zealand White rabbits at Strategic Diagnostics, Inc. (Newark DE). IgGs were purified from these antisera using Affi-Gel protein A (Bio-Rad) as recommended by Harlow and Lane (38). Anti-ChlH Δ1–823 antibodies were affinity-purified from total IgGs on ChlH Δ1–823 columns that were constructed by linking purified ChlH Δ1–823 to Affi-Gel 15 (Bio-Rad) at ~15 mg/ml. Antibodies were eluted from the ChlH Δ1–823 columns in buffer F (100 mM glycine-HCl, pH 2.5, 50% ethylene glycol) and immediately mixed with 1:10 volume of 1 M Tris-HCl, pH 8.0, as recommended by Harlow and Lane (38). Protein-containing fractions were pooled, dialyzed against phosphate-buffered saline, concentrated using Amicon Ultra-15 centrifugal filter units as described above, flash-frozen with liquid N_2, and stored at −80 °C in small aliquots.

For anti-ChlI antibody development, ChlI was expressed and purified as described for ChlH Δ1–823, except that a cDNA encoding a ChlI ORF that lacks the predicted transit peptide (ChlI Δ1–60) was amplified using CCGGAATTCGCTGTG-GCCACACTGGTCAAC and TCGCGTCGACTTATCGA-TCGATCCCTTCGATCTTGTC. ChlI Δ1–60 antibody development and affinity purification were as described for ChlH Δ1–823, except that ChlI Δ1–60, rather than ChlH Δ1–823, was linked to Affi-Gel 15.

For anti-ChlD antibody development, ChlD was expressed and purified as described for ChlH Δ1–823, except that a cDNA encoding a ChlD ORF that lacks the first 516 residues (ChlD Δ1–516) was amplified using GCGGGATCCACCCT-TAGAGCAGCTGCACCATAC and TCGCGTCGACTCAA-GAATTCTTCAGATCAGATAGTGCATCC and ligated into pHIS8-3 using BamHI and SalI. Another difference was that after elution from Ni-NTA-agarose and thrombin digestion, ChlD Δ1–516 was further purified by fractionating on a HiLoad™ 26/60 Superdex™ 200 prep-grade column equilibrated in buffer G (Tris-HCl, pH 7.9, 500 mM NaCl, 1 mM EDTA, 1 mM DTT, 10% glycerol) at 2 ml/min and at 4 °C. Anti-ChlD Δ1–516 antibodies were developed and purified as for anti-ChlH Δ1–823 and anti-ChlI Δ1–60 except that affinity purification was performed using ChlD Δ1–516 linked to Affi-Gel 10 rather than Affi-Gel 15.

All immunoblotting was done as described previously (5) using SuperSignal® West Dura extended duration substrate
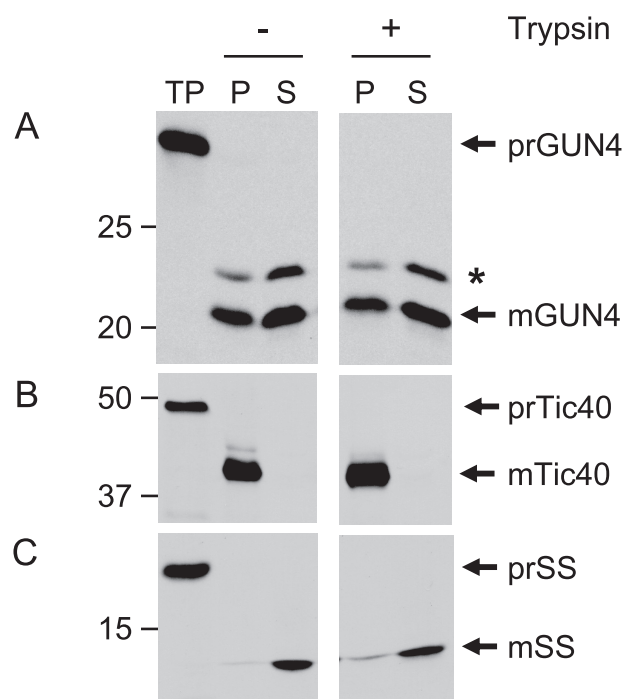

FIGURE 1. **Distribution of GUN4, Tic40, and SS in fractionated chloroplasts.** *A*, distribution of GUN4 in fractionated pea chloroplasts. ^{3}H-Labeled GUN4 leucine was imported into intact pea chloroplasts. Following the import reaction, chloroplasts were treated with (+) or without (−) trypsin. Intact chloroplasts were recovered by centrifugation through a 40% Percoll cushion, lysed, and fractionated into soluble (*S*) and membrane-containing pellet (*P*) fractions. All fractions were then analyzed by SDS-PAGE and fluorography. *TP* represents ~10% of the precursor added to an import assay. The position of the GUN4 precursor containing the transit peptide (*prGUN4*) and the major form of mature GUN4 generated by proteolytic removal of the transit peptide during import into the chloroplast (*mGUN4*) and a minor form of mature GUN4 (*) are indicated. *B*, distribution of Tic40 in fractionated pea chloroplasts. Chloroplast import and analysis were as described in *A* except that ^{35}S-labeled Tic40 was used rather than ^{3}H-labeled GUN4. *C*, distribution of SS in fractionated pea chloroplasts. Chloroplast import and analysis were as described in *A* except that ^{35}S-labeled SS was used rather than ^{3}H-labeled GUN4. Masses of protein standards are indicated at the *left* in kDa.

(Pierce). We quantified immunoreactive bands with the Versa-Doc 4000 MP and Quantity One software (Bio-Rad).

RESULTS

In Vitro Import of GUN4 into Pea Chloroplasts—To test whether the porphyrin binding activity of GUN4 affects interactions between GUN4 and chloroplast membranes, we imported GUN4 into purified pea chloroplasts *in vitro*. Because chlorophyll biosynthesis is well conserved among plant species (2, 39), we expected that GUN4 would interact similarly with proteins associated with chloroplast membranes such as ChlH from pea and Arabidopsis. The full-length GUN4 precursor containing the transit peptide was produced by *in vitro* translation. During SDS-PAGE, this translation product migrated like a 30-kDa protein (Fig. 1*A*), which was expected, based on the mass calculated from the derived amino acid sequence of GUN4 containing the predicted transit peptide (5). We tested whether GUN4 could be imported into pea chloroplasts as judged by the following: (i) a mobility shift that is consistent with the removal of the predicted 69-residue transit peptide (5), and (ii) resistance to a trypsin protease treatment, which cannot digest proteins that are transported across the inner envelope of
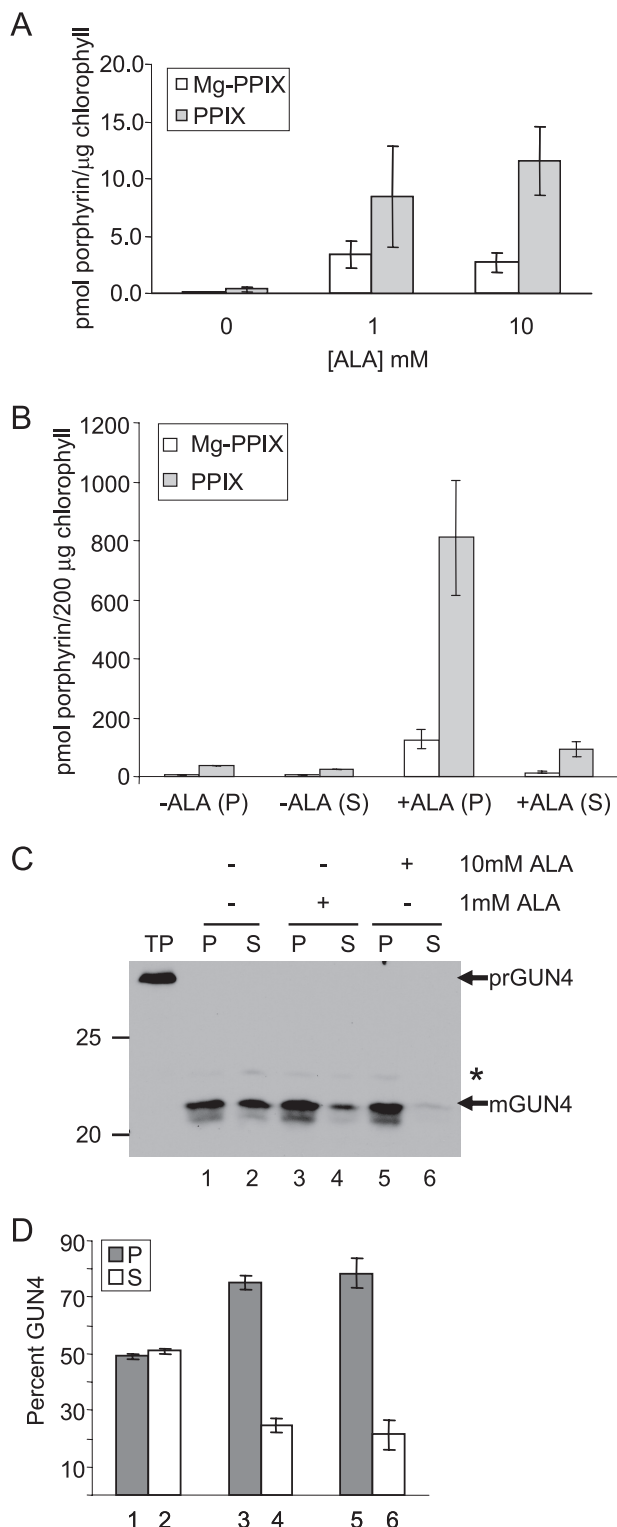
A

B

C

D

FIGURE 2. **Subchloroplastic distribution of PPIX, Mg-PPIX, and GUN4 after ALA feeding.** *A,* quantitation of PPIX and Mg-PPIX levels in ALA-fed chloroplasts. PPIX and Mg-PPIX levels were quantitated in intact chloroplasts that had been treated with 0, 1.0, or 10 mM ALA. *n* = 3. *Error bars* represent standard error. *B,* distribution of PPIX and Mg-PPIX in fractionated ALA-fed chloroplasts. Chloroplasts were fed with 10 mM ALA as in *A.* After ALA feeding, chloroplasts were lysed and separated in soluble (*S*) and membrane-containing pellet (*P*) fractions. PPIX and Mg-PPIX levels were determined in each fraction. *n* = 3. *C,* distribution of GUN4 in fractionated chloroplasts after ALA feeding. Chloroplasts were fed with ALA as described in *A.* Import and post-import analysis of GUN4 was performed as described in Fig. 1*A.* Masses of protein standards are indicated at the *left* in kDa. *D,* quantitation of GUN4 in

pea chloroplasts (26). After import into the pea chloroplast, GUN4 migrates as a doublet in SDS gels, with the predominant band migrating like a 22-kDa protein, consistent with the removal of the predicted transit peptide (Fig. 1*A*). A similar doublet was previously observed when whole cell and various chloroplast extracts from Arabidopsis were analyzed by immunoblotting with affinity-purified anti-GUN4 antibodies (5). After GUN4 was imported, chloroplasts were digested with trypsin. Intact chloroplasts were then recovered using Percoll gradients and subjected to hypotonic lysis, and the soluble and membrane-containing fractions of the chloroplast were separated by centrifugation. GUN4 was observed in both the soluble and the membrane-containing pellet fractions (Fig. 1), which indicates that GUN4 was imported into these chloroplasts and not digested by trypsin. Two control proteins, Tic40 and SS, accumulated in membrane and soluble fractions, respectively (Fig. 1, *B* and *C*), as has been demonstrated previously (23).

Subchloroplastic Distribution of GUN4 in ALA-fed Chloroplasts—To test whether porphyrin binding might affect the interactions between GUN4 and chloroplast membranes, we imported GUN4 into pea chloroplasts that were fed with ALA prior to initiating protein import. ALA feeding was previously reported to induce the levels of PPIX and Mg-PPIX in whole plants (40, 41) and to increase the levels of heme efflux from purified chloroplasts (42). Consistent with these previous reports, we found that PPIX and Mg-PPIX levels increased 20–30-fold when purified chloroplasts were fed ALA under these conditions (Fig. 2*A*) and that these porphyrins accumulated in the membrane-containing pellet fraction (Fig. 2*B*). We found that half of GUN4 associated with the membrane fraction in unfed chloroplasts, and the amount of GUN4 in the membrane fraction increased by 50% in ALA-fed chloroplasts (Fig. 2, *C* and *D*). In contrast, the distribution of Tic40 and SS did not change after ALA feeding (supplemental Fig. 1, *A* and *B*). Additionally, ALA feeding did not appear to change the total protein profile of the soluble and pellet fractions (supplemental Fig. 1*C*). ALA feeding did not affect the nature of GUN4-chloroplast membrane interactions as judged by extracting chloroplast membranes with either Na_2CO_3, pH 11, or Nonidet P-40 (supplemental Fig. 2, *A* and *B*). These data are consistent with the following: (i) elevated porphyrin levels causing GUN4 to accumulate in the membrane-containing pellet fraction after GUN4 has been imported into the chloroplast, but also with (ii) the distinct targeting of GUN4 to the stroma and to the chloroplast membranes and ALA feeding inhibiting stromal targeting. To distinguish between these possibilities, we fed ALA to chloroplasts following the import of GUN4. We found that ALA feeding subsequent to the import of GUN4 leads to increased levels of PPIX and Mg-PPIX and causes GUN4 to redistribute to the membrane-containing pellet fraction (supplemental Fig. 3, *A–C*). Based on these data, we conclude that inducing a rise in

soluble and membrane fractions after ALA feeding. The amounts of radiolabeled GUN4 in soluble (*S*) and membrane-containing pellet (*P*) fractions were quantitated in independent experiments that were performed as in *C,* using different preparations of chloroplasts. The amount of [^{3}H]GUN4 found either in the soluble (*S*) or pellet (*P*) fraction is presented as a percentage of total imported [^{3}H]GUN4. Column numbers correspond to lane numbers in *B.* *n* = 3. *Error bars* are as in *A.*
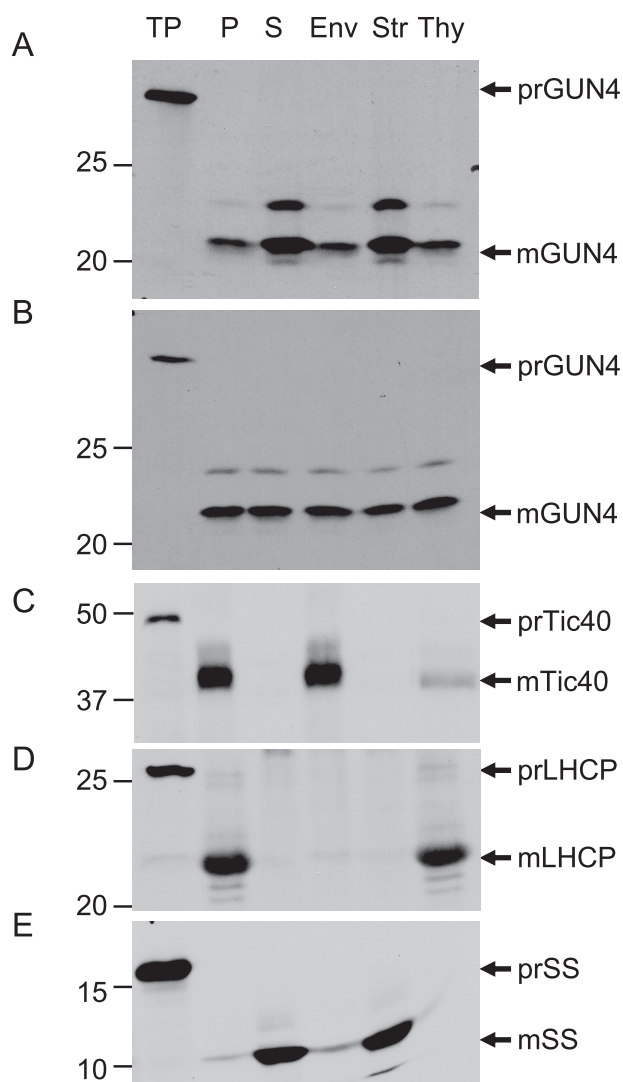
FIGURE 3. **Distribution of GUN4 in the chloroplast envelope, thylakoid, and stroma fractions after ALA feeding.** Chloroplasts were either pretreated without (*A*) or with ALA (*B*) prior to the import of [³H]GUN4. Control import assays with ALA-fed chloroplasts were likewise performed with ³⁵S-prTic40 (*C*), ³H-prLHCP (*D*), and ³⁵S-prSS (*E*). After import, chloroplasts were lysed and fractionated into soluble (*S*) and membrane-containing pellet fractions (*P*), or chloroplasts were separated into envelope (*Env*), stromal (*Str*), and thylakoid (*Thy*) fractions. All fractions were analyzed by SDS-PAGE as an equal load, using fluorography.

PPIX and Mg-PPIX levels by ALA feeding causes GUN4 to accumulate in the pellet fraction rather than blocking the import of GUN4 into the stroma.

GUN4 was previously detected in stroma, envelope, and thylakoid fractions derived from purified Arabidopsis chloroplasts (5). To test whether ALA feeding preferentially causes the accumulation of GUN4 in the chloroplast envelope or thylakoid membranes, we imported GUN4 into chloroplasts that were either fed or not fed ALA and then compared the levels of GUN4 in the stromal, envelope, and thylakoid fractions. We found that ALA feeding caused GUN4 levels to increase in the envelope and thylakoid membranes (Fig. 3, *A* and *B*). In this experiment, Tic40, LHCP, and SS accumulated in the envelope (Fig. 3*C*), thylakoids (Fig. 3*D*), and stroma (Fig. 3*E*), respectively, as reported previously (23). The levels and distributions

of Tic40, LHCP, and SS were not different from those previously reported after ALA feeding (Fig. 3, *C–E*).

To test whether the tendency of ALA to cause accumulation of GUN4 in the membrane-containing fractions was unique to the newly imported radiolabeled GUN4 or whether a similar effect might be observed with the endogenous pea GUN4, we monitored the distribution of pea GUN4 in the soluble and membrane fractions of purified pea chloroplasts after ALA feeding. We detected an immunoreactive band with essentially the same mobility as GUN4 during SDS-PAGE and found a 22% increase in the membrane-containing fraction and the same fold decrease in the soluble fraction after ALA feeding that caused PPIX and Mg-PPIX levels to increase (Fig. 4, *A–C*).

Quantitation of Porphyrin Binding by GUN4—The above findings are consistent with either porphyrin binding causing GUN4 to accumulate in the membrane-containing pellet fraction or ALA feeding somehow promoting interactions between GUN4 and chloroplast membranes by some other mechanism. To distinguish between these possibilities, we took advantage of a previous structure-function analysis of SynGUN4 (10). Based on this previous work, we made 11 single amino acid changes in GUN4 using site-directed mutagenesis (supplemental Table 2). Homologous amino acid substitutions in SynGUN4 cause general defects in porphyrin binding or specific defects in binding either DPIX or Mg-DPIX (10). We also introduced the L88F substitution from the *gun4-1* missense allele. This amino acid substitution causes the GUN4 protein to accumulate at much lower levels *in vivo* compared with the wild type. A Phe substitution at the homologous Leu residue in *T. elongatus* GUN4 and SynGUN4 causes a 6–15-fold increase in the affinities for DPIX and Mg-DPIX without affecting folding in the case of *T. elongatus* GUN4 (11). We expressed these site-directed mutants as GST fusion proteins without the predicted 69-residue transit peptide, as described previously (5). Six of these amino acid substitutions, including the L88F, caused GST-GUN4 Δ1–69 to accumulate in the insoluble fraction (supplemental Table 2) and were not analyzed further. The remaining seven amino acid substitutions did not affect the solubility of GST-GUN4 Δ1–69 in *E. coli* (supplemental Table 2) and were purified.

We determined the K_d^{DPIX} and $K_d^{\text{Mg-DPIX}}$ for GUN4 (Table 1 and supplemental Fig. 4). During the course of these studies, we observed that including 1% DMSO in binding assays does not significantly affect the K_d^{DPIX} or the $K_d^{\text{Mg-DPIX}}$ and that including 1% DMSO in binding assays solubilizes PPIX and Mg-PPIX sufficiently for us to perform binding assays with these natural ligands, which has not been reported for GUN4 from any species. We determined that the K_d^{PPIX} was almost 2-fold higher than K_d^{DPIX} and that the $K_d^{\text{Mg-PPIX}}$ was 1.5-fold lower than $K_d^{\text{Mg-DPIX}}$ (Table 1; supplemental Fig. 5).

Based on previously published biochemical and genetic data, we suggest that the major function of GUN4 *in vivo* is to stimulate Mg-PPIX biosynthesis (5, 10, 11). Nonetheless, we cannot rule out that GUN4 might participate in other reactions. To begin exploring this possibility, we tested whether GUN4 might bind other porphyrins. We performed binding assays with Mg-PPIX ME, which is the next chlorophyll precursor downstream of Mg-PPIX in the chlorophyll biosynthetic pathway. In this
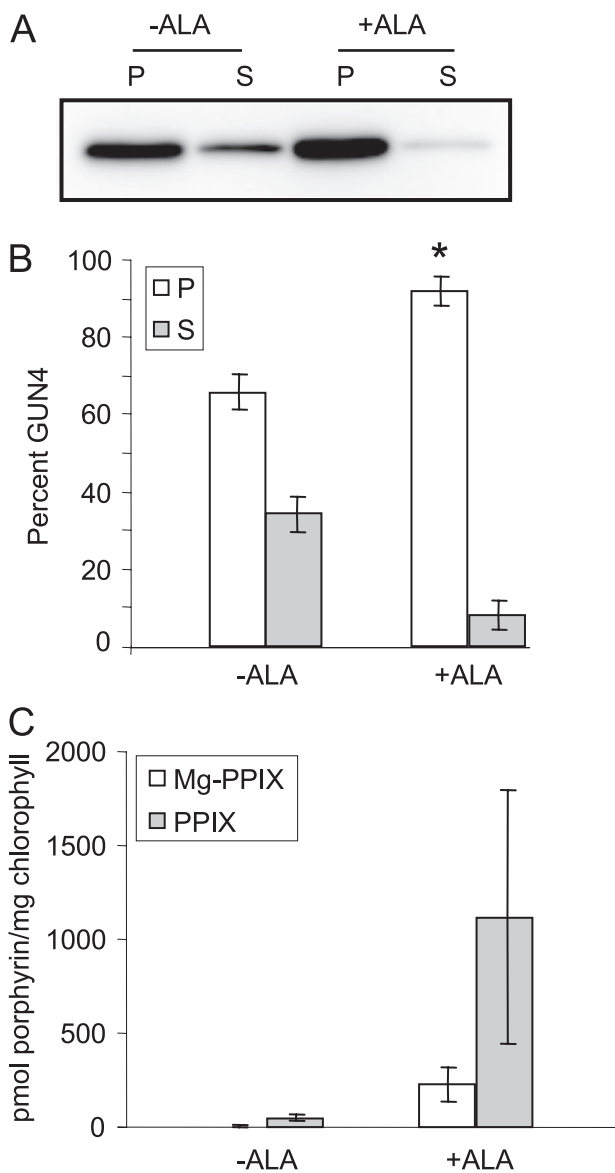
FIGURE 4. **Subchloroplastic distribution of pea GUN4 and porphyrin levels after ALA feeding.** *A,* subchloroplastic distribution of pea GUN4 following ALA feeding. Intact pea chloroplasts were either fed (+*ALA*) or not fed ALA (−*ALA*) and then subjected to a mock import assay that lacked radiolabeled proteins. These chloroplasts were subsequently lysed and fractionated. Samples of 7 μg of protein from soluble (*S*) and membrane-containing pellet (*P*) fractions were analyzed by immunoblotting with affinity-purified anti-GUN4 antibodies. *B,* quantitation of the subchloroplastic distribution of pea GUN4 after ALA feeding. $n = 5$. *Error bars* represent S.E. The statistical significance of GUN4 redistributing to the pellet during ALA feeding was tested using a paired *t* test. *Asterisk* indicates a very significant difference ($p = 0.008$). *C,* quantitation of PPIX and Mg-PPIX levels in ALA-fed chloroplasts. Porphyrin levels were quantitated as described in Fig. 2*A* after ALA feeding as described in Fig. 3, *A* and *B*. $n = 5$. *Error bars* are as in *B*.

preparation of Mg-PPIX ME, either carboxyl group is methylated in a roughly 1:1 ratio. In contrast, only the carboxyl group associated with ring *C* is methylated in nature (2). We found that the $K_d^{\text{Mg-PPIX ME}}$ was more than 2-fold higher than $K_d^{\text{Mg-PPIX}}$ (Table 1; supplemental Fig. 5). We found that GUN4 also binds uroporphyrin III, coproporphyrin III, hemin, and pheophorbide *a* (Table 1; supplemental Fig. 6) and that the affinities of GUN4 for these porphyrins are intermediate between Mg-PPIX ME and PPIX.

TABLE 1

Quantitation of porphyrin binding by GUN4

Binding reactions were performed with (+) or without (−) 1% DMSO.

Porphyrin	1% DMSO	K_d
		μM
DPIX	−	6.4 ± 0.21
DPIX	+	6.0 ± 0.39
Mg-DPIX	−	2.7 ± 0.29
Mg-DPIX	+	2.2 ± 0.30
PPIX	+	11 ± 0.50
Mg-PPIX	+	1.6 ± 0.17
Mg-PPIX ME	+	4.0 ± 0.20
Hemin	+	8.1 ± 0.75
Uroporphyrin III	+	10 ± 0.57
Coproporphyrin III	+	15 ± 0.82
Pheophorbide *a*	+	3.8 ± 0.33

TABLE 2

Quantitation of DPIX and Mg-DPIX binding by GUN4 containing the indicated amino acid substitutions

Substitution	K_d^{DPIX}	$K_d^{\text{Mg-DPIX}}$
	μM	μM
V123A	9.6 ± 0.44	8.0 ± 0.44
F191A	12 ± 0.77	7.7 ± 0.37
R211A	14 ± 0.83	14 ± 0.64

The amino acid substitutions F120W, E194A, and Q214E in GUN4 did not affect K_d^{DPIX} and $K_d^{\text{Mg-DPIX}}$.[4] The homologous substitutions (*i.e.* F132W, D199A, and R217E) significantly reduced the affinity of SynGUN4 for porphyrins (10). Amino acid substitutions V123A, F191A, and R211A caused both K_d^{DPIX} or $K_d^{\text{Mg-DPIX}}$ to increase in GUN4 (Table 2; supplemental Fig. 7, *A–C*), although the degrees of the porphyrin-binding defects were not exactly as observed for the homologous residues (*i.e.* V135A, F196A, and R214A) in SynGUN4 (10). The solubilities of PPIX and Mg-PPIX were not sufficient for us to quantitate the affinities of F191A, V123A, and R211A for these natural ligands.[4]

Subchloroplastic Distribution of GUN4 Proteins with Porphyrin-binding Defects—To test whether porphyrin-binding defects might affect interactions between GUN4 and chloroplast membranes, we imported F191A, V123A, and R211A into ALA-fed chloroplasts and fractionated these chloroplasts into soluble and membrane-containing pellet fractions. A smaller percentage of V123A associated with the membrane-containing pellet fraction compared with the wild-type GUN4, and barely detectable levels of F191A and R211A were found in the pellet fraction (Fig. 5). Additionally, and in contrast to wild-type GUN4, ALA feeding did not affect the subchloroplastic distribution of F191A, V123A, or R211A (Fig. 5).

Mg-chelatase Activity in Chloroplast Membranes of ALA-fed Chloroplasts—Because GUN4 binds ChlH and stimulates Mg-chelatase (5, 10, 11), the finding that boosting PPIX and Mg-PPIX levels in purified chloroplasts by ALA feeding causes GUN4 to accumulate in the membrane-containing pellet fraction suggests that ALA feeding might affect the Mg-chelatase activity that was previously reported to associate with pea chloroplast membranes (35). To test this idea, we assayed chloroplast membranes for Mg-chelatase after ALA feeding. Reactions were initiated by addition of PPIX dissolved in DMSO.

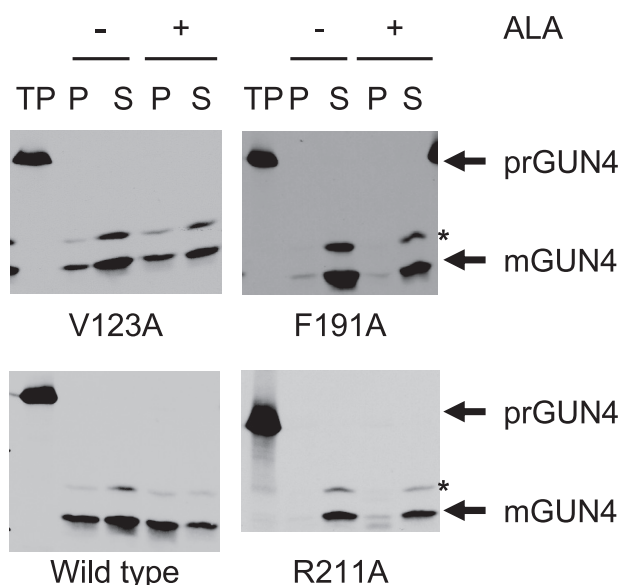[4] N. D. Adhikari, unpublished data.

FIGURE 5. **Subchloroplastic distribution of porphyrin binding-deficient GUN4 after ALA feeding.** GUN4 mutants with DPIX- and Mg-DPIX-binding defects were imported into chloroplasts that had been pretreated with or without ALA. After import, chloroplasts were lysed, fractionated, and analyzed as in Fig. 1A. The position of the GUN4 precursor containing the transit peptide (*prGUN4*), the major form of mature GUN4 generated by proteolytic removal of the transit peptide during import into the chloroplast (*mGUN4*), and a minor form of mature GUN4 (*) are indicated. Representative fluorograms from three independent experiments are shown for GUN4 containing the amino acid sequence found in wild type and for GUN4 containing the amino acid substitutions V123A, F191A, and R211A. *S,* soluble; *P,* pellet; *TP,* ~10% of the precursor added to an import assay.
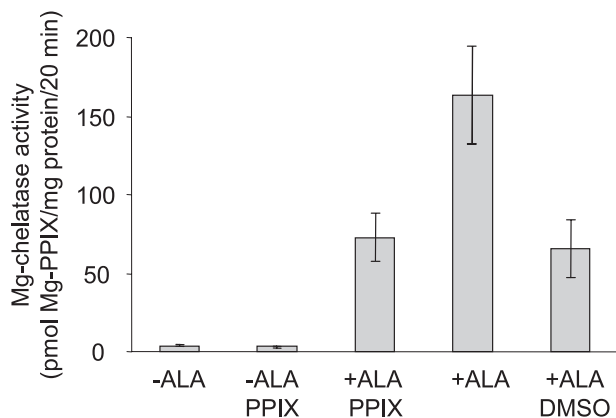

FIGURE 6. **Mg-chelatase activity associated with chloroplast membranes after ALA feeding.** Mg-chelatase assays were programmed with membranes that were isolated from chloroplasts that were either not fed (−*ALA*) or fed (+*ALA*) ALA. Mg-chelatase assays were not provided PPIX or were supplied with exogenous PPIX dissolved in DMSO (PPIX) or DMSO without PPIX (DMSO). For each set of conditions, $n \geq 3$. *Error bars* represent S.E.

When membranes derived from chloroplasts that were not fed ALA were provided or not provided PPIX, they could synthesize 4 or 3 pmol Mg-PPIX/20 min/mg protein, respectively (Fig. 6), which is 10–16-fold less activity than previously reported for pea chloroplast membranes (35). These differences may be caused by the more dilute hypotonic lysis and the distinct hypotonic lysis buffer used here, compared with that of Walker and Weinstein (35). We observed up to a 43-fold increase in Mg-chelatase activity in membranes isolated from ALA-fed chloroplasts (Fig. 6). The activity of membranes that were isolated from ALA-fed chloroplasts was reduced by more than 2-fold

when exogenous PPIX was included in these assays (Fig. 6). Additionally, we observed no significant difference in activity when membranes were assayed with the following: (i) 2% DMSO containing 1.5 μM PPIX or (ii) 2% DMSO not containing PPIX. These data indicate that Mg-chelatase does not utilize exogenous PPIX efficiently and that 2% DMSO has an inhibitory effect that is similar to PPIX dissolved in DMSO. Based on these data, we suggest that PO loads at least a fraction of the Mg-chelatase that associates with chloroplast membranes with PPIX during ALA feeding and that this preformed PPIX-Mg-chelatase complex turns over during the subsequent Mg-chelatase assay.

Subchloroplastic Distribution of Mg-chelatase Subunits in ALA-fed Chloroplasts—The elevated levels of Mg-chelatase activity in ALA-fed chloroplasts might not result solely from preloading Mg-chelatase with PPIX during ALA feeding. Porphyrins or a GUN4-porphyrin complex might contribute to this elevated level of Mg-chelatase activity by promoting the redistribution of Mg-chelatase subunits from the soluble into the membrane-containing pellet fraction. For example, a GUN4-porphyrin complex might stabilize interactions between Mg-chelatase and chloroplast membrane lipids or between Mg-chelatase and other chlorophyll biosynthetic enzymes such as PO and Mg-PPIX MT. This type of regulation would be distinct from the stimulation of Mg-chelatase activity that was previously reported for GUN4 (5, 10, 11). To begin exploring these possibilities, we monitored the levels of ChlH in these chloroplast fractions using polyclonal antibodies raised against a truncated Arabidopsis ChlH that lacks the first 823 residues and contains all of the remaining 558 carboxyl-terminal residues (hereafter referred to as ChlH Δ1–823). We found that affinity-purified anti-ChlH Δ1–823 antibodies recognize a band that was extracted from chloroplasts purified from Arabidopsis and pea that migrates like a 150-kDa protein during SDS-PAGE (supplemental Fig. 8, *A and B*). The mass of Arabidopsis ChlH calculated from the derived amino acid sequence lacking the predicted transit peptide is 144 kDa. We also found that there is a striking increase in the level of this 150-kDa protein in the Arabidopsis mutant *cch* (supplemental Fig. 8, *A and B*), which is a strong loss-of-function allele of *ChlH* (4, 43). We conclude that this band corresponds to ChlH. In four separate experiments, we observed that 40–70% of pea ChlH was in the soluble fraction of unfed chloroplasts and the remainder was in the pellet fraction. Although the distribution of ChlH in the soluble and pellet fractions was somewhat variable, we observed a statistically significant 15% increase of pea ChlH in pellet fractions after ALA feeding in each experiment (Fig. 7).

Pea ChlI was previously reported to localize mostly within the soluble fraction when purified chloroplasts from pea were lysed and fractionated (14). If ALA feeding stabilizes not only the association of GUN4 with Mg-chelatase at the site of chlorophyll biosynthesis but also interactions between Mg-chelatase and chloroplast membranes, we would expect that ChlI levels in the pellet fraction would also increase during ALA feeding. To test this idea, we monitored the levels of ChlI in these chloroplast fractions using polyclonal antibodies raised against a truncated Arabidopsis ChlI lacking the predicted 60-residue transit peptide (hereafter referred to as ChlI
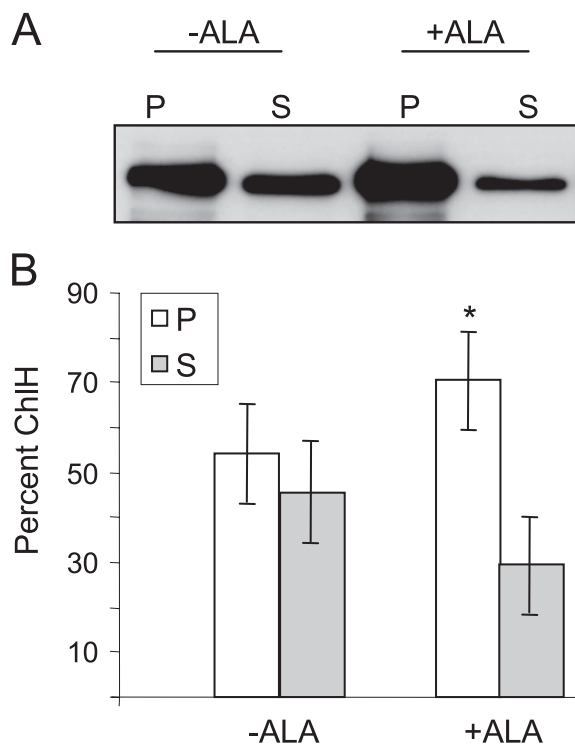
A

B

FIGURE 7. **Subchloroplastic distribution of pea ChlH after ALA feeding.** *A,* representative immunoblot showing the subchloroplastic distribution of ChlH following ALA feeding. Intact pea chloroplasts were either fed (+*ALA*) or not fed ALA (−*ALA*) and then subjected to a mock import assay that lacked a radiolabeled precursor. These chloroplasts were subsequently lysed and fractionated. 2 μg of protein from soluble (*S*) and membrane-containing pellet (*P*) fractions were analyzed by SDS-PAGE and immunoblotting with affinity-purified anti-ChlH $\Delta 1-823$ antibodies. *B,* quantitation of the subchloroplastic distribution of pea ChlH following ALA feeding. *n* = 4. *Error bars* represent S.E. The statistical significance of ChlH redistributing to the pellet during ALA feeding was tested using a paired *t* test. *Asterisk* indicates a significant difference (*p* = 0.02).

$\Delta 1-60$). We found that affinity-purified anti-ChlI $\Delta 1-60$ antibodies recognize a 43-kDa protein in extracts prepared from wild-type Arabidopsis. The mass of Arabidopsis ChlI calculated from the derived amino acid sequence lacking the predicted transit peptide is 40 kDa. We found that this immunoreactive band is present at a lower concentration in the Arabidopsis mutant *cs* (supplemental Fig. 9, *A–C*), which contains a loss-of-function allele for *ChlI* (44), and that this immunoreactive band was less than 2 kDa larger in *cs* compared with wild type (supplemental Fig. 9*B*). This decrease in mobility is consistent with the 0.8-kDa increase in the mass of the derived amino acid sequence reported for the *cs* allele (44). We conclude that our affinity-purified anti-ChlI antibodies specifically bind ChlI. These antibodies specifically recognize a single 44-kDa band in pea chloroplasts (supplemental Fig. 9*D*), which we conclude is pea ChlI. Using these affinity-purified anti-ChlI $\Delta 1-60$ antibodies, we tested the distribution of pea ChlI in the same experiments in which we observed a 15% increase in pea ChlH in the pellet fraction after ALA feeding. We found pea ChlI predominantly in the supernatant, detectable pea ChlI in the pellet, and no effect of ALA feeding on the distribution of ChlI between soluble and pellet fractions (Fig. 8*A*).

Pea ChlD was previously reported to localize in light membranes (15) that we would not expect in pellet fractions pre-
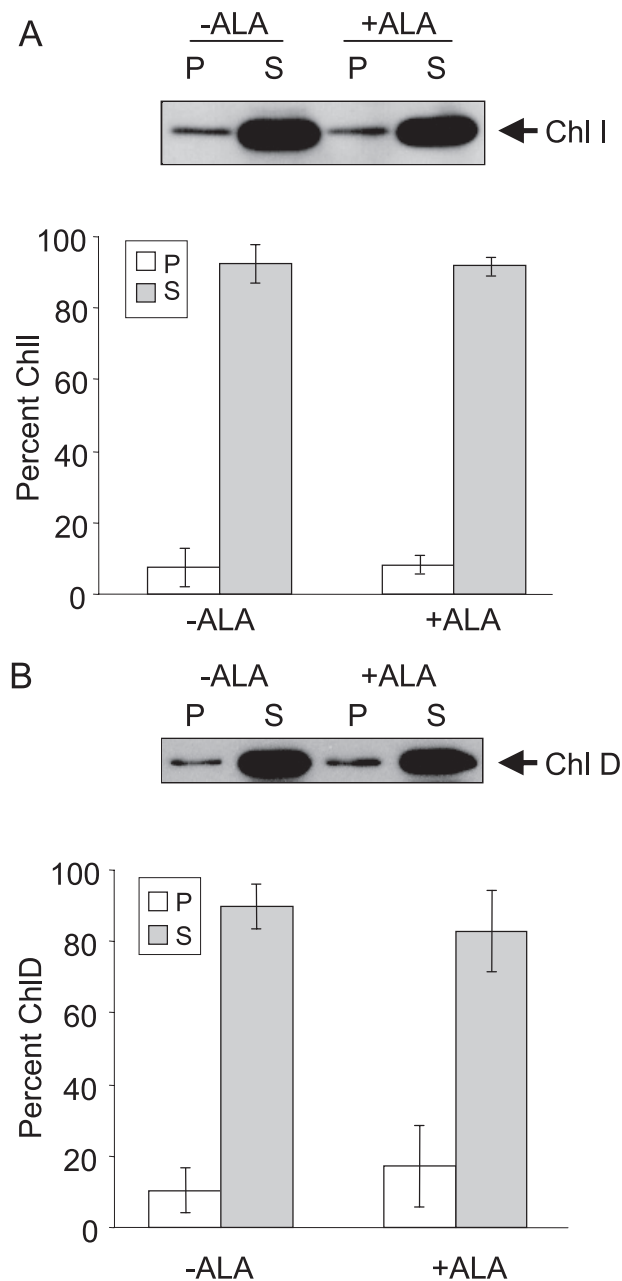
A

B

FIGURE 8. **Subchloroplastic distribution of ChlI and ChlD after ALA feeding.** *A,* subchloroplastic distribution of ChlI after ALA feeding. Intact pea chloroplasts were either fed (+*ALA*) or not fed ALA (−*ALA*) and then subjected to a mock import assay that did not contain radiolabeled proteins. These chloroplasts were subsequently lysed and fractionated. Samples of 5 μg of protein from soluble (*S*) and membrane-containing pellet (*P*) fractions were analyzed by SDS-PAGE and immunoblotting with affinity-purified anti-ChlI $\Delta 1-60$ antibodies. Immunoreactive bands from a representative experiment are shown (*top*). Immunoreactive bands were quantitated from four independent experiments prepared with different preparations of chloroplasts (*bottom*). *Error bars* represent S.E. *B,* subchloroplastic distribution of ChlD after ALA feeding. Fractions were generated and analyzed as in *A* except that immunoblotting was performed with anti-ChlD $\Delta 1-516$ antibodies. Representative immunoreactive bands are shown (*top*). Immunoreactive bands were quantitated from four independent experiments prepared with different preparations of chloroplasts (*bottom*). *Error bars* represent S.E.

pared using our experimental conditions. We monitored the levels of pea ChlD in these same chloroplast fractions using affinity-purified antibodies raised against a truncated Arabidopsis ChlD lacking the first 516 residues (hereafter referred to

TABLE 3

Quantitation of Mg-chelatase activity in supernatants prepared from lysed chloroplasts

A unit of Mg-chelatase activity produces 1 pmol of Mg-PPIX/20 min/mg protein.

Preparation	Mg-chelatase activity
	units
1	16
2	13
3	41

as ChlD Δ1–516). We found that affinity-purified anti-ChlD Δ1–516 antibodies recognize an ~94-kDa protein in Arabidopsis whole-seedling extracts. The mass of Arabidopsis ChlD calculated from the derived amino acid sequence lacking the predicted transit peptide is 79 kDa. This band is not detectable in an Arabidopsis mutant that contains a tDNA insertion in an exon of *ChlD* (supplemental Fig. 10, *A–C*). We conclude that this band is Arabidopsis ChlD. These antibodies also recognize a 93-kDa band extracted from pea chloroplasts (supplemental Fig. 10*D*), which we conclude is pea ChlD. Using these affinity-purified anti-ChlD Δ1–516 antibodies, we tested the distribution of pea ChlD in the same four independent experiments in which we observed a 22% increase in pea GUN4, a 15% increase in pea ChlH in the pellet fraction, and no change in the distribution of pea ChlI after ALA feeding. Similar to our results with pea ChlI, we found pea ChlD predominantly in the supernatant fraction and only small quantities of ChlD in the pellet fraction, regardless of whether chloroplasts were fed ALA (Fig. 8*B*).

Our data are consistent with porphyrins affecting the distribution of only GUN4 and ChlH within pea chloroplasts. Next, we tested whether the redistribution of pea GUN4 and pea ChlH from the supernatant to the pellet fractions during ALA feeding might depend on chloroplast membranes or whether these proteins might accumulate in the pellet fraction for some other reason such as a fraction of a GUN4-ChlH complex denaturing and becoming insoluble during ALA feeding. To distinguish between these possibilities, we lysed pea chloroplasts, depleted the membranes from these lysates by centrifugation, and performed Mg-chelatase assays on the resulting supernatants. We found that supernatants prepared from three independent chloroplast preparations contained from 13 to 41 units of Mg-chelatase activity (Table 3), which is similar to the activity previously reported for such supernatants (35). After performing Mg-chelatase assays with these membrane-depleted supernatants, we centrifuged these reactions using the same conditions that caused pea GUN4 and pea ChlH from lysed chloroplasts to accumulate in the membrane-containing pellet fraction. We found that in contrast to the results that we obtained with lysed chloroplasts, pea GUN4 and pea ChlH remained entirely within the supernatant fraction when Mg-chelatase reactions were performed with membrane-depleted supernatants (Fig. 9).

Subchloroplastic Distribution of GUN4 and Mg-chelatase Subunits in Chloroplasts Fed with Various Porphyrins—We expected that PPIX and Mg-PPIX would stabilize interactions between chloroplast membranes and the GUN4 and ChlH proteins because PPIX and Mg-PPIX are the only porphyrin substrate and product of Mg-chelatase and because ChlH and GUN4 are not known to catalyze other reactions. Nonetheless,
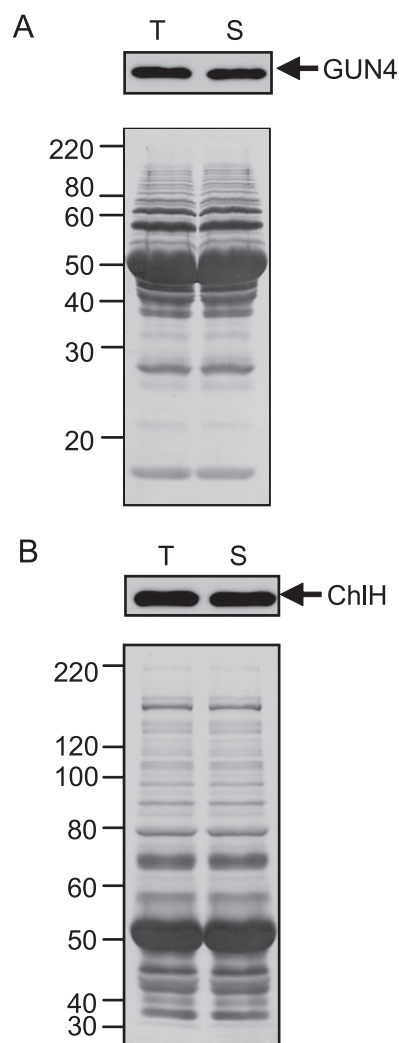

FIGURE 9. **Solubility of pea GUN4 and pea ChlH in chloroplast-membrane-depleted Mg-chelatase assays.** *A*, solubility of pea GUN4 in chloroplast membrane-depleted Mg-chelatase assays. Mg-chelatase assays that contained a total volume of 300 μl were programmed with supernatants from lysed chloroplasts. After a 20-min Mg-chelatase reaction, 40 μl of the reaction was removed (*T*). The reactions were then centrifuged at 16,000 × *g* for 10 min at 4 °C, and 40 μl of the supernatant (*S*) was removed. All fractions were analyzed by immunoblotting with affinity-purified anti-GUN4 antibodies (*top*). Polyvinylidene difluoride membranes were stained with Coomassie Blue after immunoblotting (*bottom*). *B*, solubility of pea ChlH in chloroplast-membrane-depleted Mg-chelatase assays. Fractions were prepared as in *A* and were analyzed by immunoblotting with affinity-purified anti-ChlH Δ1–823 antibodies (*top*). Polyvinylidene difluoride membranes were stained with Coomassie Blue after immunoblotting (*bottom*).

our finding that GUN4 can bind a variety of porphyrins implies that GUN4 binding any of these ligands might cause a redistribution of GUN4 from the soluble to the membrane-containing pellet fraction. We expected that chloroplasts would take up PPIX and other porphyrins *in vitro* and that GUN4 might bind these porphyrins after they are taken up because purified chloroplasts were reported previously to synthesize Mg-PPIX from exogenous PPIX (36, 45, 46). To test this idea, we fed pea chloroplasts with various porphyrins that GUN4 binds and monitored the distribution of GUN4 in soluble and membrane-containing fractions by immunoblotting. We found that similar to feeding chloroplasts ALA, feeding chloroplasts PPIX, Mg-PPIX, uroporphyrin III, coproporphyrin III, hemin, or phe-
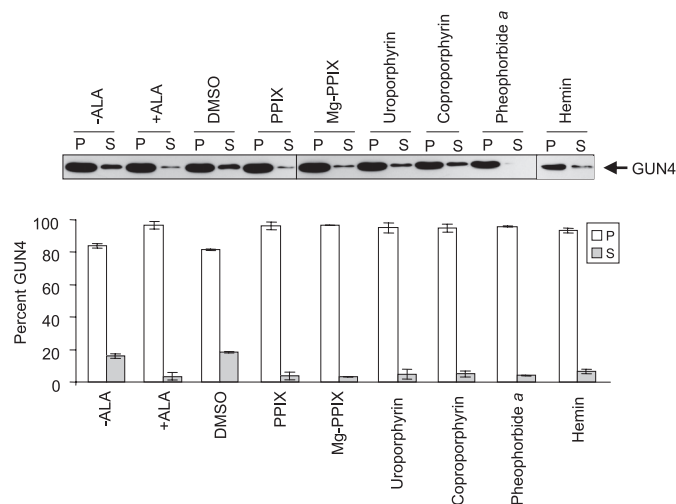
FIGURE 10. **Subchloroplastic distribution of GUN4 after feeding with ALA or various porphyrins.** Pea chloroplasts were incubated in import buffer lacking ALA (−*ALA*), containing ALA (+*ALA*), containing 2% DMSO (*DMSO*), or 20 μM of the indicated porphyrin and 1–2% DMSO. Next, the chloroplasts were subjected to a mock import assay that lacked a radiolabeled precursor. Chloroplasts were lysed and fractionated. Soluble (*S*) and membrane-containing pellet (*P*) fractions were analyzed by immunoblotting with affinity-purified anti-GUN4 antibodies. A representative immunoblot is shown (*top*). Immunoreactive bands were quantitated in fractions derived from at least two independent preparations of chloroplasts (*bottom*). *Error bars* represent S.E.

ophorbide *a* caused GUN4 to accumulate in the pellet fraction (Fig. 10).

DISCUSSION

GUN4 was previously localized to the thylakoid and envelope membranes but was found mostly in the soluble fraction of chloroplasts that were purified from fully expanded rosette leaves of Arabidopsis (5). Here we report a roughly 50:50 distribution, or that GUN4 predominantly associates with the membrane-containing fraction depending on whether GUN4 was imported or pea GUN4 was monitored in 6–8-day-old pea leaves. Differences in the affinities of GUN4 and pea GUN4 for chloroplast membranes or differences in the chlorophyll biosynthetic capacities of fully expanded and young rapidly growing leaves may account for these differences. Consistent with the relatively higher rate of chlorophyll biosynthesis in young leaves stabilizing interactions between GUN4 and chloroplast membranes, we found that feeding ALA to purified chloroplasts causes a striking increase in the biosynthesis of PPIX and Mg-PPIX and also causes both GUN4 and ChlH to accumulate in the membrane-containing fraction at the expense of the soluble fraction. Although we cannot rule out possibilities such as porphyrin binding causing a rapid redistribution of GUN4, ChlH, or a GUN4-ChlH complex from the chloroplast stroma to the chloroplast membranes, this possibility seems unlikely because of the high viscosity of the chloroplast stroma (47). The most parsimonious interpretation of our data is as follows: (i) most of GUN4 and ChlH associate with chloroplast membranes; (ii) a fraction of GUN4, ChlH, or a GUN4-ChlH complex dissociates from chloroplast membranes and accumulates in the soluble fraction during chloroplast lysis and fractionation; and (iii) the porphyrin-bound conformations of GUN4

and ChlH have higher affinities for either chloroplast membrane lipids and/or chlorophyll biosynthetic enzymes that more stably associate with chloroplast membranes such as PO and Mg-PPIX MT.

Although GUN4-porphyrin complexes were previously reported to stimulate Mg-chelatase activity (5, 10, 11), our findings suggest that GUN4 might regulate chlorophyll biosynthesis on another level. We propose that GUN4 or a GUN4-porphyrin complex helps to stabilize interactions between ChlH and chloroplast membranes (*i.e.* the site of chlorophyll biosynthesis), which was not previously reported for GUN4. Complexes of chlorophyll biosynthetic enzymes that include Mg-chelatase have been reported or suggested because Mg-chelatase and Mg-PPIX MT can convert PPIX to Mg-PPIX ME *in vitro* without appreciable accumulation of Mg-PPIX (48) and because ChlH stimulates Mg-PPIX MT (49–51). However, all Mg-PPIX does not appear to be efficiently channeled through a complex composed of Mg-chelatase and Mg-PPIX MT because Mg-PPIX accumulates in green Arabidopsis seedlings (52, 53). We propose that GUN4 binds at least a fraction of the Mg-PPIX that accumulates *in vivo* by itself or as part of a GUN4-ChlH complex. GUN4 may be necessary if Mg-chelatase-Mg-PPIX complexes are unstable or if a fraction of active ChlH does not associate with Mg-PPIX MT and might help prevent the photosensitizing chlorophyll precursors from causing photooxidative damage.

These findings may contribute to our understanding of the competition between Mg-chelatase and ferrochelatase for PPIX. By stabilizing complexes of enzymes that contain Mg-chelatase, GUN4 might help divert PPIX from heme biosynthesis and into chlorophyll biosynthesis. Both PO and ferrochelatase stably associate with chloroplast membranes (16–19, 54) and have been predicted to form a complex based on their crystal structures (55). Porphyrin-bound GUN4 might help Mg-chelatase compete with ferrochelatase for interactions with PO, thereby helping to divert PPIX from heme to chlorophyll biosynthesis. Alternatively, if Mg-chelatase and ferrochelatase utilize separate pools of PPIX, as has been suggested (56), we would expect that GUN4 would affect only chlorophyll biosynthesis.

Complexes of cooperating enzymes are expected to limit active site access of exogenously supplied substrates (57, 58). Consistent with this idea, we found that exogenously supplied PPIX did not stimulate Mg-chelatase activity in our membrane-containing pellet fraction but that PPIX derived from ALA feeding caused a striking increase in Mg-chelatase activity. Pea chloroplast membranes were previously reported to contain low levels of Mg-chelatase activity when assayed with exogenous PPIX. Reactions lacking exogenous PPIX were not previously reported (35). The striking increase in Mg-chelatase activity caused by ALA feeding likely results from the 22% increase in GUN4 and the 15% increase in ChlH in the chloroplast membranes, along with the preloading of ChlH or a GUN4-ChlH complex with PPIX. Our finding that, in contrast to GUN4 and ChlH, ALA feeding does not stabilize interactions between chloroplast membranes and either ChlI or ChlD suggests that these Mg-chelatase subunits do not have a higher affinity for the porphyrin-bound form of ChlH or at least that

such a difference cannot be detected with the chloroplast lysis and fractionation assay described here. The low levels of ChlI and ChlD that we observed in the pellet fraction likely explain the low Mg-chelatase activity that we and Walker and Weinstein (35) observed in membrane-containing pellet fractions relative to reactions programmed with both soluble and membrane-containing fractions (35).

K_d^{DPIX} and $K_d^{Mg-DPIX}$ have been reported for SynGUN4 and *T. elongatus* GUN4 (5, 10, 11), but only qualitative porphyrin-binding experiments were previously reported for GUN4 (5). We found similarities and differences in the porphyrin-binding constants of GUN4 and its cyanobacterial relatives. Like its cyanobacterial relatives (5, 10, 11), GUN4 has a higher affinity for Mg-DPIX than DPIX, but GUN4 has a 3–10-fold lower affinity for these porphyrins than its cyanobacterial relatives. K_d^{PPIX} and $K_d^{Mg-PPIX}$ had not been reported previously for GUN4 or any cyanobacterial relatives of GUN4. We found that including 1% DMSO in binding assays did not significantly affect K_d^{DPIX} and $K_d^{Mg-DPIX}$ but promoted the solubility of PPIX and Mg-PPIX, thereby allowing us to determine K_d^{PPIX} and $K_d^{Mg-PPIX}$, which resembled K_d^{DPIX} and $K_d^{Mg-DPIX}$, respectively. GUN4 has a slightly higher affinity for Mg-PPIX than for Mg-DPIX and has an almost 2-fold lower affinity for PPIX than for DPIX. The higher affinity of SynGUN4 for metalated porphyrins was previously attributed to these porphyrins assuming a planar conformation in contrast to unmetalated porphyrins, which assume a more puckered or ruffled conformation (10). Our findings indicate that this preference for metalated porphyrins is more striking for the natural ligands than for the deuteroporphyrins, and we suggest that the vinyl groups that distinguish PPIX from DPIX contribute to this binding selectivity. This finding may at least partially explain why K_m^{DPIX} is lower than K_m^{PPIX} in lysed pea chloroplasts (14).

SynGUN4 was previously shown to bind a variety of porphyrins with K_d values that range from 0.26 to 11 μM (5, 10, 11). Here we report that GUN4 can bind nine different porphyrins with K_d values ranging from 1.6 to 15 μM. Most of the porphyrins that we analyzed are found in plants or are oxidized versions of porphyrins and porphyrinogens found in plants. Although the only difference in Mg-PPIX and hemin is a chelated magnesium or ferric ion, we found that GUN4 binds Mg-PPIX with a 5-fold higher affinity than hemin. SynGUN4 was previously reported to bind cobalt(III) PPIX with an almost 2-fold higher affinity than hemin (10). Thus, like SynGUN4, GUN4 can distinguish between derivatives of PPIX that contain distinct metal ions. Modifications of the porphyrin ring were also reported to affect the affinities of SynGUN4 for porphyrins (10). Arg-214 of SynGUN4 is conserved as Arg-211 in GUN4. In SynGUN4, Arg-214 resides in the $\alpha6/\alpha7$ loop that lies loosely across the "palm" region of the cupped hand domain and makes a major contribution to porphyrin binding, presumably by interacting with one of the carboxyl moieties of DPIX and Mg-DPIX (10). Methylation of a carboxyl moiety in Mg-PPIX ME could lower the affinities of both GUN4 and SynGUN4 for this porphyrin. Indeed, we observed that $K_d^{Mg-PPIX ME}$ was 2.5-fold higher than $K_d^{Mg-PPIX}$. However, because either the carboxyl moiety of the commercially available Mg-PPIX ME used here is methylated rather than the carboxyl moiety attached only to

ring C, as observed in nature, these data do not unambiguously establish that GUN4 binds Mg-PPIX ME with a lower affinity than Mg-PPIX. GUN4 binding uroporphyrin III, coproporphyrin III, hemin, and pheophorbide *a* indicates that GUN4 is similar to SynGUN4 in that GUN4 can bind a variety of porphyrins with diverse ring substituents (10). Moreover, we found that feeding uroporphyrin III, coproporphyrin III, hemin, or pheophorbide *a* to chloroplasts causes pea GUN4 to accumulate in the membrane-containing pellet fraction. These data lend further support to a model in which a porphyrin-bound conformation of GUN4 has an elevated affinity for chloroplast membranes. The finding that binding a variety of porphyrins promotes interactions between GUN4 and chloroplast membranes implies that GUN4 could be involved in other reactions besides the Mg-chelatase reaction. However, previous analyses of *gun4* mutants are consistent with GUN4 not having a major role in the metabolism of porphyrinogens and other porphyrins besides PPIX and Mg-PPIX. *gun4* mutants are chlorophyll-deficient (4, 5, 59); *gun4* nulls are albino under optimal growth conditions but viable when they are provided sucrose (5). Although these phenotypes are expected for mutants that cannot synthesize chlorophyll, we expect that mutants with severe defects in plastid heme metabolism would exhibit more severe or lethal phenotypes regardless of whether sucrose is provided. Additionally, *gun4* mutants were not reported to exhibit lesions (4, 5, 59) like those present in mutants with reduced levels of uroporphyrinogen III decarboxylase and coproporphyrinogen III oxidase (60–62). Moreover, although we found that GUN4 binds pheophorbide *a*, an early intermediate in chlorophyll catabolism, we observed that *gun4* mutants do not exhibit phenotypes like those with defects in the enzymes that degrade chlorophyll such as the stay-green phenotype (63, 64, 65) (supplemental Fig. 11). From these data we conclude that GUN4 does not appear to promote chlorophyll catabolism. In summary, although GUN4 can bind diverse porphyrins *in vitro* and binding any of these porphyrins causes GUN4 to more stably associate with chloroplast membranes, the simplest interpretation of these new data and previous analyses of *gun4* mutants is that the major function of GUN4 *in vivo* is to promote the biosynthesis of Mg-PPIX and to bind Mg-PPIX.

Several amino acid substitutions that do not affect the solubility of His-tagged SynGUN4 expressed in *E. coli* appear to cause GST-GUN4 $\Delta1$–69 to accumulate as inclusion bodies. Species-specific differences in stability, or technical explanations such as the use of different tags, may explain these apparent differences in solubility. Among the seven amino acid substitutions that did not cause GST-GUN4 $\Delta1$–69 to accumulate in inclusion bodies, only V123A, F191A, and R211A reduced the affinity of GUN4 for porphyrins. The finding that four amino acid substitutions inhibit porphyrin binding in SynGUN4 but not GUN4 is consistent with species specificity in particular binding determinants or in indirect effects on binding. Val-123 in GUN4 is homologous to Val-135 in SynGUN4. In SynGUN4, Val-135 contributes to a concave and hydrophobic surface referred to as the "greasy palm" of the cupped hand domain (10). Phe-191 in GUN4 is homologous to Phe-196 in SynGUN4. Like Arg-214 of SynGUN4, Phe-196 resides on the $\alpha6/\alpha7$ loop, which lies across the greasy palm (10). Because

V123A, F191A, and R211A elevate K_d^{DPIX} and $K_d^{\mathrm{Mg\text{-}DPIX}}$, we expected that these amino acid substitutions would also impair the porphyrin-mediated interactions between GUN4 and chloroplast membranes. Indeed, we found that much less V123A, F191A, and R211A associated with membranes. However, because we found that these amino acid substitutions impair rather than abolish binding, and because ALA feeding causes a striking increase in PPIX and Mg-PPIX, we expected that ALA feeding might stabilize interactions between these proteins and chloroplast membranes, thereby causing more V123A, F191A, and R211A to accumulate in the membrane-containing pellet fraction. However, we found that ALA feeding could not stabilize interactions between chloroplast membranes and V123A, F191A, or R211A. These data are consistent with pea GUN4 competing much more effectively with V123A, F191A, and R211A relative to wild-type GUN4. These data are also consistent with V123A, F191A, and R211A not only affecting porphyrin binding but also directly or indirectly affecting interactions between GUN4 and other molecules that might tether GUN4 to chloroplast membranes such as ChlH.

The L88F substitution derived from the *gun4-1* missense allele causes the GUN4 protein to accumulate at much lower levels than in wild-type Arabidopsis, as judged by immunoblotting (5). The homologous amino acid substitution in *T. elongatus* GUN4 does not cause misfolding and causes a striking decrease in the K_d^{DPIX} and $K_d^{\mathrm{Mg\text{-}DPIX}}$ for *T. elongatus* GUN4 and SynGUN4. Together, these data provide evidence that GUN4 might be degraded more rapidly when bound to porphyrins. However, the observation that the L88F substitution promotes insolubility of GST-GUN4 Δ1–69 expressed in *E. coli* reported here suggests that, in Arabidopsis, less GUN4 accumulates in *gun4-1* because of protein instability caused by misfolding, as suggested previously (5), rather than from protein instability caused by a striking increase in the affinities for porphyrins.

In summary, our major finding is that porphyrin binding helps stabilize interactions between GUN4 and possibly ChlH with chloroplast membranes. Based on these data, we suggest that porphyrins and/or GUN4-porphyrin complexes might stabilize interactions between ChlH and chloroplast membranes, thereby facilitating the channeling of porphyrins into chlorophyll biosynthesis. These findings support a model in which GUN4-porphyrin complexes promote chlorophyll biosynthesis not only by stimulating Mg-chelatase activity but also by affecting interactions between ChlH and chloroplast membranes.

REFERENCES

1. Stephenson, P. G., and Terry, M. J. (2008) *Photochem. Photobiol. Sci.* **7,** 1243–1252
2. Tanaka, R., and Tanaka, A. (2007) *Annu. Rev. Plant Biol.* **58,** 321–346
3. Susek, R. E., Ausubel, F. M., and Chory, J. (1993) *Cell* **74,** 787–799
4. Mochizuki, N., Brusslan, J. A., Larkin, R., Nagatani, A., and Chory, J. (2001) *Proc. Natl. Acad. Sci. U.S.A.* **98,** 2053–2058
5. Larkin, R. M., Alonso, J. M., Ecker, J. R., and Chory, J. (2003) *Science* **299,** 902–906
6. Wilde, A., Mikolajczyk, S., Alawady, A., Lokstein, H., and Grimm, B. (2004) *FEBS Lett.* **571,** 119–123
7. Sobotka, R., Dühring, U., Komenda, J., Peter, E., Gardian, Z., Tichy, M., Grimm, B., and Wilde, A. (2008) *J. Biol. Chem.* **283,** 25794–25802
8. Masuda, T. (2008) *Photosynth. Res.* **96,** 121–143
9. Elmlund, H., Lundqvist, J., Al-Karadaghi, S., Hansson, M., Hebert, H., and Lindahl, M. (2008) *J. Mol. Biol.* **375,** 934–947
10. Verdecia, M. A., Larkin, R. M., Ferrer, J. L., Riek, R., Chory, J., and Noel, J. P. (2005) *PLoS Biol.* **3,** e151
11. Davison, P. A., Schubert, H. L., Reid, J. D., Iorg, C. D., Heroux, A., Hill, C. P., and Hunter, C. N. (2005) *Biochemistry* **44,** 7603–7612
12. Nakayama, M., Masuda, T., Bando, T., Yamagata, H., Ohta, H., and Takamiya, K. (1998) *Plant Cell Physiol.* **39,** 275–284
13. Gibson, L. C., Marrison, J. L., Leech, R. M., Jensen, P. E., Bassham, D. C., Gibson, M., and Hunter, C. N. (1996) *Plant Physiol.* **111,** 61–71
14. Guo, R., Luo, M., and Weinstein, J. D. (1998) *Plant Physiol.* **116,** 605–615
15. Luo, M., Weinstein, J. D., and Walker, C. J. (1999) *Plant Mol. Biol.* **41,** 721–731
16. van Lis, R., Atteia, A., Nogaj, L. A., and Beale, S. I. (2005) *Plant Physiol.* **139,** 1946–1958
17. Lermontova, I., Kruse, E., Mock, H. P., and Grimm, B. (1997) *Proc. Natl. Acad. Sci. U.S.A.* **94,** 8895–8900
18. Che, F. S., Watanabe, N., Iwano, M., Inokuchi, H., Takayama, S., Yoshida, S., and Isogai, A. (2000) *Plant Physiol.* **124,** 59–70
19. Watanabe, N., Che, F. S., Iwano, M., Takayama, S., Yoshida, S., and Isogai, A. (2001) *J. Biol. Chem.* **276,** 20474–20481
20. Block, M. A., Tewari, A. K., Albrieux, C., Maréchal, E., and Joyard, J. (2002) *Eur. J. Biochem.* **269,** 240–248
21. Mohapatra, A., and Tripathy, B. C. (2007) *Photosynth. Res.* **94,** 401–410
22. Umesono, K., Murakami, K. K., Thompson, C. C., and Evans, R. M. (1991) *Cell* **65,** 1255–1266
23. Tripp, J., Inoue, K., Keegstra, K., and Froehlich, J. E. (2007) *Plant J.* **52,** 824–838
24. Olsen, L. J., and Keegstra, K. (1992) *J. Biol. Chem.* **267,** 433–439
25. Bruce, B. D., Perry, S., Froehlich, J., and Keegstra, K. (1994) in *Plant Molecular Biology Manual* (Gelvin, S. B., and Schilperoort, R. B., eds) pp. J1:1–15, Kluwer Academic Publishers, Norwell, MA
26. Jackson, D. T., Froehlich, J. E., and Keegstra, K. (1998) *J. Biol. Chem.* **273,** 16583–16588
27. Eichwurzel, I., Stiel, H., and Röder, B. (2000) *J. Photochem. Photobiol. B* **54,** 194–200
28. Rebeiz, C. A. (2002) in *Heme, Chlorophyll, and Bilins* (Smith, A. G., and Witty, M., eds) pp. 111–155, Humana Press Inc., Totowa, NJ
29. Rimington, C. (1960) *Biochem. J.* **75,** 620–623
30. Brown, S. B., and Lantzke, I. R. (1969) *Biochem. J.* **115,** 279–285
31. Keegstra, K., and Yousif, A. E. (1986) *Methods Enzymol.* **118,** 316–325
32. Sambrook, J., and Russell, D. W. (2001) *Molecular Cloning: A Laboratory Manual*, 3rd Ed., Cold Spring Harbor Laboratory Press, Cold Spring Harbor, NY
33. Karger, G. A., Reid, J. D., and Hunter, C. N. (2001) *Biochemistry* **40,** 9291–9299
34. Kuzmic, P. (1996) *Anal. Biochem.* **237,** 260–273
35. Walker, C. J., and Weinstein, J. D. (1991) *Proc. Natl. Acad. Sci. U.S.A.* **88,** 5789–5793
36. Walker, C. J., and Weinstein, J. D. (1991) *Plant Physiol.* **95,** 1189–1196
37. Jez, J. M., Ferrer, J. L., Bowman, M. E., Dixon, R. A., and Noel, J. P. (2000) *Biochemistry* **39,** 890–902
38. Harlow, E., and Lane, D. (1999) *Using Antibodies: A Laboratory Manual*, pp. 70–80, Cold Spring Harbor Laboratory Press, Cold Spring Harbor, NY
39. Eckhardt, U., Grimm, B., and Hörtensteiner, S. (2004) *Plant Mol. Biol.* **56,** 1–14
40. Gough, S. (1972) *Biochim. Biophys. Acta* **286,** 36–54
41. Granick, S. (1961) *J. Biol. Chem.* **236,** 1168–1172
42. Thomas, J., and Weinstein, J. D. (1990) *Plant Physiol.* **94,** 1414–1423
43. Espineda, C. E., Linford, A. S., Devine, D., and Brusslan, J. A. (1999) *Proc. Natl. Acad. Sci. U.S.A.* **96,** 10507–10511

44. Koncz, C., Mayerhofer, R., Koncz-Kalman, Z., Nawrath, C., Reiss, B., Redei, G. P., and Schell, J. (1990) *EMBO J.* **9,** 1337–1346

45. Fuesler, T. P., Wright, L. A., and Castelfranco, P. A. (1981) *Plant Physiol.* **67,** 246–249

46. Fufsler, T. P., Castelfranco, P. A., and Wong, Y. S. (1984) *Plant Physiol.* **74,** 928–933

47. Köhler, R. H., Schwille, P., Webb, W. W., and Hanson, M. R. (2000) *J. Cell Sci.* **113,** 3921–3930

48. Jensen, P. E., Gibson, L. C., Shephard, F., Smith, V., and Hunter, C. N. (1999) *FEBS Lett.* **455,** 349–354

49. Shepherd, M., McLean, S., and Hunter, C. N. (2005) *FEBS J.* **272,** 4532–4539

50. Hinchigeri, S. B., Hundle, B., and Richards, W. R. (1997) *FEBS Lett.* **407,** 337–342

51. Johnson, E. T., and Schmidt-Dannert, C. (2008) *J. Biol. Chem.* **283,** 27776–27784

52. Mochizuki, N., Tanaka, R., Tanaka, A., Masuda, T., and Nagatani, A. (2008) *Proc. Natl. Acad. Sci. U.S.A.* **105,** 15184–15189

53. Strand, A., Asami, T., Alonso, J., Ecker, J. R., and Chory, J. (2003) *Nature* **421,** 79–83

54. Suzuki, T., Masuda, T., Singh, D. P., Tan, F. C., Tsuchiya, T., Shimada, H., Ohta, H., Smith, A. G., and Takamiya, K. (2002) *J. Biol. Chem.* **277,** 4731–4737

55. Koch, M., Breithaupt, C., Kiefersauer, R., Freigang, J., Huber, R., and Messerschmidt, A. (2004) *EMBO J.* **23,** 1720–1728

56. Cornah, J. E., Terry, M. J., and Smith, A. G. (2003) *Trends Plant Sci.* **8,** 224–230

57. Winkel, B. S. (2004) *Annu. Rev. Plant Biol.* **55,** 85–107

58. Jørgensen, K., Rasmussen, A. V., Morant, M., Nielsen, A. H., Bjarnholt, N., Zagrobelny, M., Bak, S., and Møller, B. L. (2005) *Curr. Opin. Plant Biol.* **8,** 280–291

59. Vinti, G., Hills, A., Campbell, S., Bowyer, J. R., Mochizuki, N., Chory, J., and López-Juez, E. (2000) *Plant J.* **24,** 883–894

60. Mock, H. P., and Grimm, B. (1997) *Plant Physiol.* **113,** 1101–1112

61. Mock, H. P., Heller, W., Molina, A., Neubohn, B., Sandermann, H., Jr., and Grimm, B. (1999) *J. Biol. Chem.* **274,** 4231–4238

62. Ishikawa, A., Okamoto, H., Iwasaki, Y., and Asahi, T. (2001) *Plant J.* **27,** 89–99

63. Schelbert, S., Aubry, S., Burla, B., Agne, B., Kessler, F., Krupinska, K., and Hörtensteiner, S. (2009) *Plant Cell* **21,** 767–785

64. Pruzinská, A., Tanner, G., Aubry, S., Anders, I., Moser, S., Müller, T., Ongania, K. H., Kräutler, B., Youn, J. Y., Liljegren, S. J., and Hörtensteiner, S. (2005) *Plant Physiol.* **139,** 52–63

65. Park, S. Y., Yu, J. W., Park, J. S., Li, J., Yoo, S. C., Lee, N. Y., Lee, S. K., Jeong, S. W., Seo, H. S., Koh, H. J., Jeon, J. S., Park, Y. I., and Paek, N. C. (2007) *Plant Cell* **19,** 1649–1664